arXiv:1908.01314v1 [cs.LG] 4 Aug 2019

MoGA: Searching Beyond MobileNetV3

Xiangxiang Chu, Bo Zhang, Ruijun Xu

Xiaomi AI Lab

{chuxiangxiang, zhangbo11, xuruijun}@xiaomi.com

Abstract

The evolution of MobileNets has laid a solid foundation for neural network application on the mobile end. With the latest MobileNetV3, neural architecture search again claimed its supremacy on network design. Till today all mobile methods mainly focus on CPU latency instead of GPU, the latter, however, has lower overhead and interference and is much preferred in the industry. To mitigate this gap, we propose the first Mobile GPU-Aware (MoGA) neural architecture search in order to be precisely tailored for real-world applications. Further, the ultimate objective to devise a mobile network lies in achieving better performance by maximizing the utilization of bounded resources. While urging higher capability and restraining time consumption, we unconventionally encourage increasing the number of parameters for higher representational power. Undoubtedly, these three forces are not reconcilable and we have to alleviate the tension by weighted evolution techniques. Lastly, we deliver our searched networks at a mobile scale that outperform MobileNetV3 under the similar latency constraints, i.e., MoGA-A achieves 75.9% top-1 accuracy on ImageNet, MoGA-B meets 75.5% which costs only 0.5ms more on mobile GPU than MobileNetV3, which scores 75.2%. MoGA-C best attests GPU-awareness by reaching 75.3% and being slower on CPU but faster on GPU. The models and test code is made available here [1][2].

1 Introduction

The MobileNets trilogy has opened a gate to on-device artificial intelligence for the mobile vision world (Howard et al. 2017; Sandler et al. 2018; Howard et al. 2019). In the meantime, neural architecture search becomes the new engine to power the future architecture innovation (Zoph et al. 2018; Tan et al. 2019; Cai, Zhu, and Han 2019; Chu et al. 2019a). The guideline in designing mobile architecture is that not only should the high performance be concerned, but also we must strive for low latency in favor of rapid responsiveness and improved power efficiency to prolong battery life.

In this paper, we aim to bring forward the frontier of mobile neural architecture design by stretching out the representational space within the desired latency range. First, we make a shift in the search trend from mobile CPU to GPU,

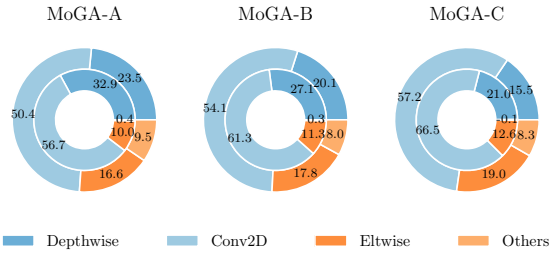

Figure 1: Latency pie chart of MoGA-A, B, C operations when run on mobile CPUs (inner circle with TFLite) vs. on GPUs (outer circle with MACE). Best viewed in color.

with which we can gauge the speed of a model more accurately and provide a production-ready solution. On this account, our overall search approach is named Mobile GPU-Aware neural architecture search (MoGA). Our results suggest that generated models show different behavior related to the targeted hardware as shown in Figure 1. Second, while considering accuracy, latency and the number of parameters as our objectives, particular care is required to abate these three contending forces. One important insight is that the number of parameters should be made reasonably large instead of as few as possible, this leverages performance but doesn't necessarily increase latency. At the mobile scale, this would be the proper choice as we try to avoid underfitting instead of overfitting. On top of that, as we care more about accuracy and latency than the number of parameters, we replace traditional multi-objective optimization with a weighted fitness strategy. Finally, we present our searched architectures MoGA-A that achieves 75.9% top-1 accuracy on ImageNet, MoGA-B 75.5% and MoGA-C 75.3%. MoGA-C is best comparable to MobileNetV3, with similar FLOPs and an equal number of parameters, which runs slower on CPUs but faster on GPUs.

The paper is structured as follows. We first summarize the related works in Section 2. We then show motivations for our Mobile GPU-aware NAS approach in Section 3. The overall approach is later extensively discussed in Section 4. Experiments on supernet training and ImageNet classification are presented in Section 5. Section 6 gives a short analysis of

[1]https://github.com/xiaomi-automl/MoGA

[2]This is a preview version, subject to frequent changes.

our experiments. Section 7 holds our conclusions and future work.

2 Related Works

During the era of human craftsmanship, MobileNetV1 and V2 (Howard et al. 2017; Sandler et al. 2018) have widely disseminated depthwise separable convolutions and inverted residuals with linear bottlenecks. Squeeze and excitation blocks are later introduced in (Hu, Shen, and Sun 2018) for residual modules in ResNet (He et al. 2016).

In their aftermath, a series of automated architectures are searched based on these building blocks (Tan et al. 2019; Cai, Zhu, and Han 2019; Chu et al. 2019a; Howard et al. 2019). For instance, MnasNet frames a factorized hierarchical search space with the mobile inverted bottleneck convolution blocks (MB) of variable kernel sizes and expansion rates, its latest variation also includes an option of squeeze and excitation module (SE) (Tan et al. 2019). Proxyless-NAS and FairNAS adopt a similar design (Cai, Zhu, and Han 2019; Chu et al. 2019a) without SE modules, while MobileNetV3 achieves a new state of the art by integrating SE within MnasNet search space, along with numerous techniques like Platform-Aware NAS (Tan et al. 2019), NetAdapt (Yang et al. 2018) and improved non-linearities (Howard et al. 2019).

As for search methods, recent attention has been drawn to the one-shot approach initiated by (Bender et al. 2018), as it tremendously reduces computing resources and also offers state of the art results (Cai, Zhu, and Han 2019; Stamoulis et al. 2019; Guo et al. 2019; Chu et al. 2019a). Briefly, the one-shot approach embodies weight-sharing across models by constructing a supernet where each step of training accounts for the final performance. Its single-path variations further cut down memory consumption by training a picked path instead of a whole supernet, yielding more flexibility for architecture design (Stamoulis et al. 2019; Guo et al. 2019; Chu et al. 2019a). Among them, FairNAS proved it is critical to maintaining strict fairness for training single-path nets so to reach a steady rank, which can reasonably facilitate the search process (Chu et al. 2019a).

3 Mobile GPU-Aware NAS Based on Multi-Objective Optimization

In this section, we draw insights from the development of MobileNets and experiments on mobile GPU/CPU relationship to better formulate our design problem.

3.1 Mobile GPU Awareness

Recent NAS approaches have an increased emphasis on target platforms, primarily on mobile CPUs (Tan et al. 2019; Dong et al. 2018; Wu et al. 2019; Cai, Zhu, and Han 2019; Stamoulis et al. 2019; Howard et al. 2019). MnasNet has developed a reward $ACC \times (LAT/TAR)^w$, which requires delicate manual tuning for a parameter w to balance between latency and accuracy (Tan et al. 2019), in MobileNetV3, w is reduced from -0.07 to -0.15 (Howard et al. 2019) to compensate for accuracy drop.

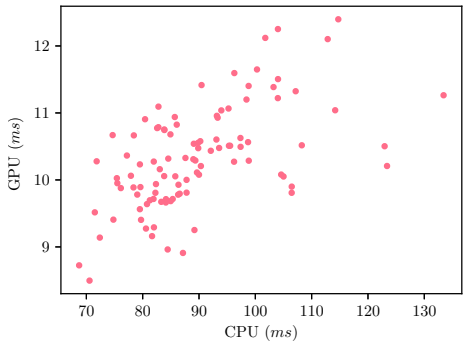

Figure 2: Latency relationship on CPUs vs. on GPUs.

In practice, mobile neural networks are mostly deployed to run on GPUs, DSPs and recently also on specific Neural Processing Units (NPUs), while CPUs would be the last to choose. To further investigate the relationship of CPU latencies versus GPU ones, we measure 100 random models on both two platforms, and the result is shown in Figure 2. We see that there is no obvious linear correspondence. Hence, To develop architectures with target hardware in mind is more than necessary. For this reason, we are driven to apply Mobile GPU awareness to the latest neural architecture search approaches.

3.2 Underfitting and Overfitting

As we try to tear apart two contradicting objectives, there isn't too much freedom left to increase accuracy with a constrained latency. We observe from the evolution of MobileNets as in Figure 3, the number of parameters has grown while the latencies and multiply-adds are kept low.

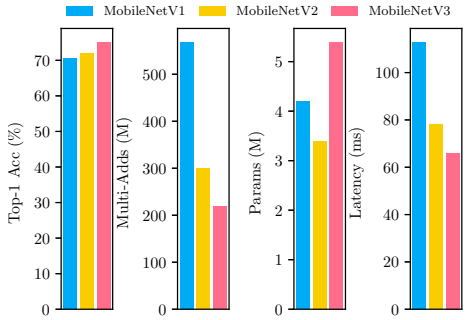

Figure 3: The evolution of MobileNets.

Moreover, for the mobile end, models tend to be underfitted instead of overfitted since they carry fewer numbers of parameters (Zhang et al. 2018), which means we are free to encourage representational power by enlarging its range of parameters. This intuition greatly expands our design space.

Index	Expansion	Kernel Size	SE
0	3	3	-
1	3	3	✓
2	3	5	-
3	3	5	✓
4	3	7	-
5	3	7	✓
6	6	3	-
7	6	3	✓
8	6	5	-
9	6	5	✓
10	6	7	-
11	6	7	✓

Table 1: Each layer in our search space has 12 choices.

3.3 Problem Formulation

Most hardware aware methods build the classification problem as follows,

$$\begin{aligned} \max \quad & Accuracy(m) \\ s.t. \quad & Latency(m) < L \\ & model \quad m \in S. \end{aligned} \tag{1}$$

In Equation 1, S is the whole search space and L is a given maximal acceptable latency[3]. Informally speaking, larger models have greater capacity and to achieve better accuracy. Therefore, NAS methods will prefer models which have large running time. The whole NAS pipeline muse be rerun to adapt a changing requirement of L.

Search Space Our search space is built layer by layer on inverted bottleneck blocks as (Cai, Zhu, and Han 2019; Chu et al. 2019a). We keep the same number of layers and activation functions as MobilenetV3-large. For each layer, we search from three dimensions (see Table 1):

- the convolution kernel size (3, 5, 7)
- the expansion ratio for the inverted bottleneck block (3, 6)
- whether the squeezing and excitation mechanism is enabled or not.

Therefore, the total search space has a volume of 12^{14}, which needs efficient methods to differentiate better models from worse. To be simple, we search for the expansion rate instead of channels which is used by (Howard et al. 2019) based on NetAdapt (Yang et al. 2018). Besides, we utilize choice index to directly encode each model chromosome. More formally, a model chromosome m can be written as $m_1 = (x_1^1, x_2^1, ..., x_{14}^1)$.

To address the above problem, a recent popular approach formulate it as multi-objective problem (MOP) whose solution is called Pareto Front,

$$\begin{aligned} max \quad & \{Accuracy(m), -Latency(m)\} \\ & m \in S. \end{aligned} \tag{2}$$

One popular approach for Equation 2 is converting it into a customized weighted product objective $ACC \times (LAT/TAR)^w$, which requires delicate manual tuning for a parameter w to balance between latency and accuracy (Tan et al. 2019).

As inspired by Section 3.2, we also maximize the number of parameters in addition to the two objectives in Equation 2. More formally, we try to solve the following problem,

$$\begin{aligned} max \quad & \{Accuracy(m), -Latency(m), Params(m)\} \\ & m \in S. \end{aligned} \tag{3}$$

As a matter of fact, these three objectives are not of equal importance in most cases. A typical case is like Equation 2. Therefore, we need to introduce some strategies to address the issue. Let $w_{acc}, w_{lat}, w_{params}$ denote customized preference for those objectives. Without loss of generality, the problem can be defined as,

$$\begin{aligned} min \quad & \{-Accuracy(m), Latency(m), -Params(m)\} \\ s.t. \quad & m \in S \\ & w_{acc} + w_{lat} + w_{params} = 1 \\ & w_{acc}, w_{lat}, w_{params} >= 0. \end{aligned} \tag{4}$$

There are two basic subproblems to be solved in the next section. One is to instantly evaluate any model's accuracy and latency, the other is to solve Equation 4. We use NSGA-II, which is one of the most powerful and widely used algorithms to solve such problems (Deb et al. 2002), mainly for two reasons. First, it's efficient to solve MOPs, especially when the number of objectives is large, some variants can still work. Second, it's flexible to apply customized preferences for different objectives and to handle various constraints. We also benefit from its implicit objective scaling and normalization.

4 Solving it Using Weighted NSGA-II

4.1 Accuracy and Latency Prediction

The evaluation of model accuracy must be made immediate for searching efficiency. We take advantage of a variation of One-Shot approach FairNAS (Chu et al. 2019a) for fast evaluation with a stable ranking. Unlike their version, based on our previously defined search space, we construct a supernet with 12 choice blocks per layer. Then we train our supernet on ImageNet dataset with the same fairness strategy. We observe a steady convergence even with doubled choices, as shown in Figure 4.

As for mobile GPU latency, since each choice block in our search space has a fixed input, we can efficiently approximate the latency for any sampled model. To do so, we benchmark the latency of each choice block under a given input and construct a layerwise lookup table. We can then accurately calculate the latency simply by accumulating time cost across all layers. We find that predicted GPU latency coincides with ground-truth and has much smaller RMSE, see Figure 5.

We don't utilize real-time latency acquisition during the pipeline from a cell phone for two reasons. One is that while

[3]The following latency means mobile GPU latency.

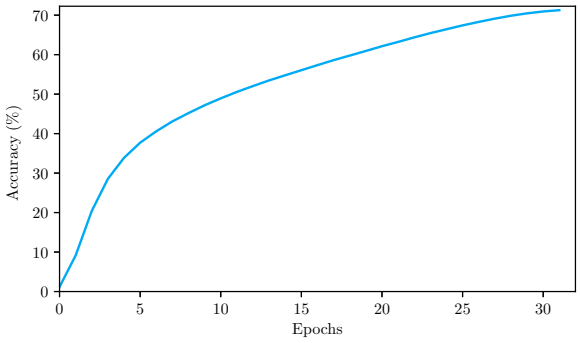

Figure 4: Fair training of our supernet with 12 choice blocks per layer.

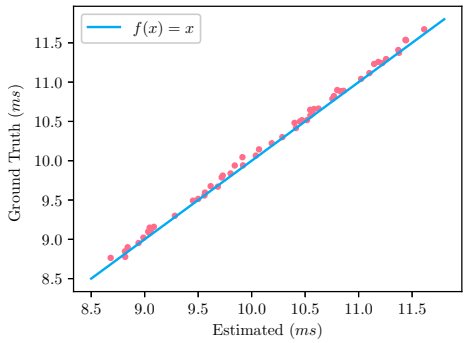

Figure 5: Mobile GPU latency measured vs. predicted ones. The latency RMSE is 0.0571ms.

the performance of each selected submodel can be rapidly predicted by the supernet which takes less than 1 minute, it will easily become the bottleneck when we use a mobile phone to evaluate latency on the fly. The other is that latency measurement may become inaccurate as a result of overheating after long-time insistent testing.

4.2 Weighted NSGA-II

We comply with the standard NSGA-II procedure, and only state something different if essential.

Population Initialization We initialize population to introduce various choice blocks to encourage exploration.

Crossover To be simple, we use single-point crossover. To be specific, for two models $m_1 = (x_1^1, x_2^1, ..., x_{14}^1)$ and $m_2 = (x_1^2, x_2^2, ..., x_{14}^2)$, if the point position is k, the result after crossover is $(x_1^1, x_2^1, ...x_k^2..., x_{14}^1)$.

Mutation We use hierarchical mutation and the same hyperparameters as (Chu et al. 2019b).

Non-dominated Sorting For a minimization problem with n objectives, we state that A dominates B means for any objective O_i, $O_{iA} \leq O_{iB}$. For a given population P, A is not dominated if and only if A is not dominated by any other individuals.

The crowding distance is a key component to achieve better trade-off among various objectives. We use the customized weights to define the crowding distance for non-boundary individuals,

$$D(m_j) = \sum_{i=1}^{n} w_i * \frac{O^i_{neighbor+} - O^i_{neighbor-}}{O^i_{max} - O^i_{min}}. \quad (5)$$

Note $O^i_{neighbour-}$ and $O^i_{neighbor+}$ are the i-th objective value of the left and the right neighbor of m_j respectively, while O^i_{max} and O^i_{min} are the maximum and the minimum for the i-th objective in the current population. In Equation 5, customized preference is flexibly incorporated. If $w_{acc} = w_{lat} = w_{params} = \frac{1}{3}$, it degrades as the standard NSGA-II. In our experiment, $w_{acc} = w_{lat} = 0.4, w_{params} = 0.2$.

4.3 Pipeline

Our search pipeline is pictured as an evolution process. We have a trained supernet as a fast evaluator, a GPU latency lookup table, and a statistic tool to compute the number of parameters. The initial random population thus propagates at a significant speed. We can digram our pipeline as in Figure 6.

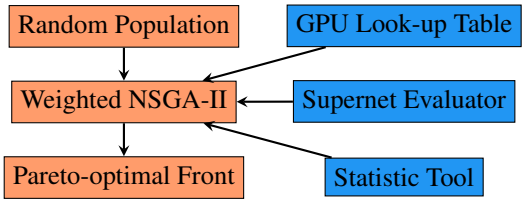

Figure 6: The overall pipeline of MoGA.

5 Experiments

5.1 Mobile GPU Latency

Specifically, we employ Mobile AI Compute Engine (MACE) for mobile GPU benchmarking (Xiaomi 2018). We sample some models randomly and report the differences between our predictions and on-device measurement, which is shown in Figure 5. For instant latency prediction, we construct a latency lookup table based on MACE measurements on all 12 choices blocks for each cell (12×14). For the final comparison with state-of-the-art models, we also report mobile GPU latencies with SNPE (Qualcomm 2019), and CPU latencies with Tensorflow Lite (Abadi et al. 2015). Considering recent updates on Tensorflow speed up the inference time, we choose a version that can reproduce the result on MobileNetV2 (Sandler et al. 2018).

5.2 Training

Training our supernet We search on the ImageNet (Deng et al. 2009) classification dataset directly. We take out 50k images from the training set to form our validation set and use the official validation set as our test set to evaluate our models, on par with other methods. In particular, we train the supernet by SGD with 0.9 momentum for 32 epochs. The average accuracies per epoch are plotted in Figure 4. The initial learning rate is 0.05 and is scheduled to arrive at zero within a single cosine cycle. This search stage takes about 12 GPU days.

Training for Stand-Alone models To alleviate the training unfairness, we utilize the same training tricks and hyperparameters as MobileNetV3 (Howard et al. 2019). By doing so, we singled out various training tricks in order to focus on the authentic model performance. Linear warm-up (Goyal et al. 2017) is applied for the first 5 epochs. We use a dropout rate of 0.2 before the last layer (Srivastava et al. 2014) and L2 weight decay $1e-5$. Besides, we perform all our experiments on two Tesla-V100 machines.

6 Results

6.1 Comparisons with Various State-of-the-art Methods

We are mostly comparable to the latest version of MnasNet (Tan et al. 2019) and MobileNetV3 (Howard et al. 2019), as we share similar search space. Also, we use the same training and data processing tricks as in (Tan et al. 2019) for a full training of stand-alone models. Note that with latency considered as one of the objectives, our generated models pay more attention to increase the number of parameters in order to gain higher performance, see detailed comparison results in Table 3.

For a fair comparison, here we only consider single branch models based on inverted bottleneck blocks. Our MoGA-A achieves a new state-of-the-art top-1 accuracy 75.9%, surpassing Proxyless-R Mobile (+1.3%), MnasNet-A1 (+0.7%), MnasNet-A2 (+0.3%) with fewer FLOPs. Our MoGA-B obtains 75.5%, excelling MobileNetV3 at similar GPU speed. MoGA-C hits a higher accuracy with a faster GPU speed, note it is slower on CPU, which otherwise will be treated as inferior by CPU-aware methods. Therefore, it's beneficial to fit models for specific hardware, indicating that even latency on other computing units and FLOPs are not ideal proxies.

MoGA-A makes extensive use of large kernels (4 layers with 7×7), which helps to enlarge the receptive field. Moreover, it places the most large kernels on the stage with 14×14 input to reduce the speed cost. It also utilizes a large expansion rate after each downsampling stage to keep and extract more useful features.

As for MoGA-B, the expansion rates across various layers mimic a sine curve. Like MoGA-A, it utilizes five 7×7 kernels to obtain a large receptive field. To cut down the latency cost, it places most of them in the 14×14 stage. Like FairNAS-A, it selects larger expansion rates before downsampling operations.

It's interesting to see that both MoGA-C and MobileNetV3-large simply contain 3×3 and 5×5 kernels only. Moreover, they utilize the same amount of 3×3 and 5×5 layers. While MobileNetV3-large prefers 5×5 operations in the tail of the model, MoGA-C chooses 3×3. Besides, MoGA-C places 5×5 kernels in the middle and uses less squeeze-and-excitation operations. In such way, it better balances accuracy and speed.

6.2 Mobile GPU Awareness Analysis

We benchmark the inference cost for our three models both on mobile CPUs and GPUs. The result is shown in Figure 1. As for mobile GPUs, all models spend most of the time on 2D convolutions. MoGA-A and B spend the second most of the time on depthwise convolutions because they make extensive use of large kernels and expansion rates, whereas MoGA-C pays much attention to elementwise operations instead.

It is worth noticing that how models exhibit a different behavior on mobile GPUs than on CPUs. For instance, vanilla convolutions and depthwise convolutions generally take bigger percentages on CPUs than on GPUs, while elementwise operations have a smaller percentage, as seen from Figure 1. Additionally, there is a discrepancy when running the same model with the different inference frameworks as well (Table 3), which could call for a framework-aware solution. Apart from the mobile framework we use, CPUs and GPUs differ on inherent microarchitectures, which puts hardware-specific requirements a must for the design of neural architectures.

6.3 Ablation Study

Model Selection We compare the hierarchical weighted NSGA-II with the random baseline in Figure 7. Plenty of models from the baseline are dominated by the hierarchical version.

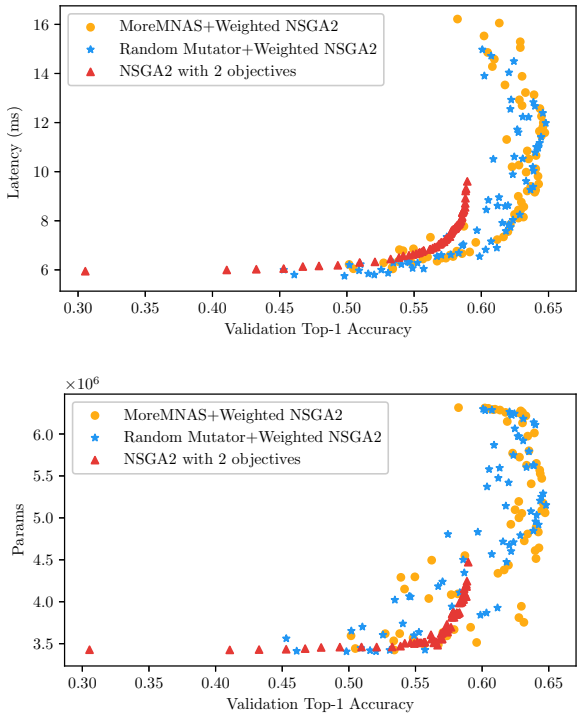

Figure 7: Pareto-Front of MoreMNAS with weighted NSGA-II compared with that of a random mutator and of two objectives (accuracy, latency).

Does it matter to use parameters as an objective? We compare the best elitists for Equation 2 and 4, which is shown in the upper part of Figure 7. The Pareto front formed

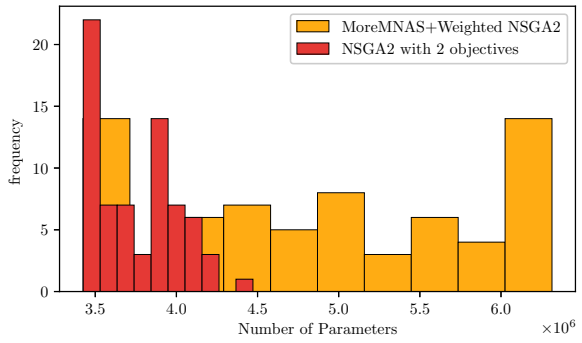

Figure 8: Histogram of number of parameters of models from the last generation of MoreMNAS with weighted NSGA-II compared with that of two objectives (accuracy, latency).

by the two objectives is largely surrounded by those with three.

While FairNAS (Chu et al. 2019a) states that a fair training can boost the rank relationship between the supernet predictor and stand-alone training, it also points out that it can be affected by initialization techniques and suboptimal training hyperparameters. For the latter, we empirically maximize the number of parameters as a compensation bonus. Occam's Razor doesn't fit in this case, because in such mobile setting, a neural network is prone to underfitting instead of overfitting. Without this compensation or minimizing the number of parameters, NSGA-II is at risk of excluding models with more parameters generation by generation. For evidence, we show the histograms of the number of parameters for the final elitists in Figure 8.

7 Conclusion

To sum up, we have discussed several critical issues in mobile neural architecture design. First, we promote the first Mobile GPU-Aware (MoGA) solution, as in production, running networks on GPUs are much preferred for their faster speed and lower overhead. Previous works are centered on CPUs which could introduce inaccuracies. Second, while overfitting is not the concern for networks at mobile scale, we attempt to liberate the representational power other than to suppress it to fit other constraints. Weighted fitness strategy is then adopted to comfort more valuable objectives. Lastly, we employ an automated search approach on adapted search space based on MnasNet and MobileNetV3, which generates a new set of state-of-the-art architectures for mobile settings. Namely, MoGA-A obtains 75.9% top-1 accuracy on ImageNet, and MoGA-B 75.5%, MoGA-C 75.3%. Note that MoGA-C outperforms MobileNetV3 with competing mobile GPU latency with similar FLOPs and an equal number of parameters.

In the future, there will still be continuous interest to squeeze out better performance within limited hardware bounds, especially on targeted computing units. Also, balancing between architecture diversity and search space size will remain as a major topic, it also poses a challenge for searching algorithms when search space grows enormously.

Input	Ops	t	c	SE	NL	s
$224^2 \times 3$	conv2d, 3×3	-	16	-	HS	2
$112^2 \times 16$	bneck, 3×3	1	16	-	RE	1
$112^2 \times 16$	bneck, 5×5	6	24	-	RE	2
$56^2 \times 24$	bneck, 7×7	6	24	-	RE	1
$56^2 \times 24$	bneck, 3×3	6	40	✓	RE	2
$28^2 \times 40$	bneck, 3×3	6	40	✓	RE	1
$28^2 \times 40$	bneck, 3×3	3	40	✓	RE	1
$28^2 \times 40$	bneck, 3×3	6	80	-	HS	2
$14^2 \times 80$	bneck, 3×3	6	80	-	HS	1
$14^2 \times 80$	bneck, 7×7	6	80	-	HS	1
$14^2 \times 80$	bneck, 7×7	3	80	✓	HS	1
$14^2 \times 80$	bneck, 7×7	6	112	-	HS	1
$14^2 \times 112$	bneck, 3×3	6	112	-	HS	1
$14^2 \times 112$	bneck, 3×3	6	160	-	HS	1
$14^2 \times 112$	bneck, 5×5	6	160	✓	HS	2
$7^2 \times 160$	bneck, 5×5	6	160	✓	HS	1
$7^2 \times 160$	conv2d, 1×1	-	960	-	HS	1
$7^2 \times 960$	avgpool, 7×7	-	-	-	HS	-
$1^2 \times 960$	conv2d, 1×1	-	1280	-	HS	1
$1^2 \times 1280$	conv2d, 1×1	-	k	-		-

Table 2: The architecture of MoGA-A. Note t, c, s refer to expansion rate, output channel size and stride respectively. SE for squeeze-and-excitation, NL for non-linearity.

References

[Abadi et al. 2015] Abadi, M.; Agarwal, A.; Barham, P.; Brevdo, E.; Chen, Z.; Citro, C.; Corrado, G. S.; Davis, A.; Dean, J.; Devin, M.; Ghemawat, S.; Goodfellow, I.; Harp, A.; Irving, G.; Isard, M.; Jia, Y.; Jozefowicz, R.; Kaiser, L.; Kudlur, M.; Levenberg, J.; Mané, D.; Monga, R.; Moore, S.; Murray, D.; Olah, C.; Schuster, M.; Shlens, J.; Steiner, B.; Sutskever, I.; Talwar, K.; Tucker, P.; Vanhoucke, V.; Vasudevan, V.; Viégas, F.; Vinyals, O.; Warden, P.; Wattenberg, M.; Wicke, M.; Yu, Y.; and Zheng, X. 2015. TensorFlow: Large-scale machine learning on heterogeneous systems. tag: v1.14.0-rc0. Software available from tensorflow.org.

[Bender et al. 2018] Bender, G.; Kindermans, P.-J.; Zoph, B.; Vasudevan, V.; and Le, Q. 2018. Understanding and simplifying one-shot architecture search. In *International Conference on Machine Learning*, 549–558.

[Cai, Zhu, and Han 2019] Cai, H.; Zhu, L.; and Han, S. 2019. Proxylessnas: Direct neural architecture search on target task and hardware. In *International Conference on Learning Representations*.

[Chu et al. 2019a] Chu, X.; Zhang, B.; Xu, R.; and Li, J. 2019a. Fairnas: Rethinking evaluation fairness of weight sharing neural architecture search. *arXiv preprint arXiv:1907.01845*.

[Chu et al. 2019b] Chu, X.; Zhang, B.; Xu, R.; and Ma, H.

Methods	Mult-Adds (M)	Params (M)	Lat_g^{SNPE} (ms)	Lat_g^{MACE} (ms)	Lat_c (ms)	Top-1 (%)	Top-5 (%)
MobileNetV2 1.0 (Sandler et al. 2018)	300	3.4	6.9†	7.0†	78	72.0	91.0
MobileNetV3 Large 1.0 (Howard et al. 2019)	219	5.4	10.8⋆	9.5⋆	70 (66)⋆	75.0 (75.2)⋆	92.2
MnasNet -A1(Tan et al. 2019)	312	3.9			78	75.2	92.5
MnasNet-A2 (Tan et al. 2019)	340	4.8			84	75.6	92.7
FBNet-B (Wu et al. 2019)	295	4.5			23 ‡	74.1	
Proxyless-R Mobile (Cai, Zhu, and Han 2019)	320†	4.0	7.3†	7.9†	87 (78)†	74.6	92.2
Proxyless GPU (Cai, Zhu, and Han 2019)	465†	7.1	9.6†	9.8†	126 (124)†	75.1	-
Single-Path NAS (Stamoulis et al. 2019)	365	4.3			79	75.0	92.2
FairNAS-A (Chu et al. 2019a)	388	4.6	9.8†	9.7†	104	75.3	92.4
MoGA-A (Ours)	304	5.1	11.8	11.1	101	**75.9**	92.8
MoGA-B (Ours)	248	5.5	10.3	10.0	81	75.5	92.6
MoGA-C (Ours)	221	5.4	9.6	8.8	71	75.3	92.5

Table 3: Comparison of mobile models on ImageNet. The input size is set to 224×224. ⋆: Our implementation with the stated hyperparameters. Numbers within the parentheses are reported by its authors, same for below. †: Based on its published code. Mobile CPU latencies are measured on a Google Pixel 1 using a single large core of CPU with a batch size of 1 (via Tensorflow Lite shipped with Tensorflow). Mobile GPU latencies are benchmarked both with SNPE and MACE on a Mi MIX 3.‡: Time measured by its author on a Samsung Galaxy S8.

2019b. Multi-objective reinforced evolution in mobile neural architecture search. *arXiv preprint arXiv:1901.01074*.

[Deb et al. 2002] Deb, K.; Pratap, A.; Agarwal, S.; and Meyarivan, T. 2002. A fast and elitist multiobjective genetic algorithm: Nsga-ii. *IEEE transactions on evolutionary computation* 6(2):182–197.

[Deng et al. 2009] Deng, J.; Dong, W.; Socher, R.; Li, L.-J.; Li, K.; and Fei-Fei, L. 2009. Imagenet: A large-scale hierarchical image database. In *Proceedings of the IEEE Conference on Computer Vision and Pattern Recognition*, 248–255. Ieee.

[Dong et al. 2018] Dong, J.-D.; Cheng, A.-C.; Juan, D.-C.; Wei, W.; and Sun, M. 2018. Dpp-net: Device-aware progressive search for pareto-optimal neural architectures. In *Proceedings of the European Conference on Computer Vision (ECCV)*, 517–531.

[Goyal et al. 2017] Goyal, P.; Dollár, P.; Girshick, R.; Noordhuis, P.; Wesolowski, L.; Kyrola, A.; Tulloch, A.; Jia, Y.; and He, K. 2017. Accurate, large minibatch sgd: Training imagenet in 1 hour. *arXiv preprint arXiv:1706.02677*.

[Guo et al. 2019] Guo, Z.; Zhang, X.; Mu, H.; Heng, W.; Liu, Z.; Wei, Y.; and Sun, J. 2019. Single path one-shot neural architecture search with uniform sampling. *arXiv preprint arXiv:1904.00420*.

[He et al. 2016] He, K.; Zhang, X.; Ren, S.; and Sun, J. 2016. Deep residual learning for image recognition. In *Proceedings of the IEEE Conference on Computer Vision and Pattern Recognition*, 770–778.

[Howard et al. 2017] Howard, A. G.; Zhu, M.; Chen, B.; Kalenichenko, D.; Wang, W.; Weyand, T.; Andreetto, M.; and Adam, H. 2017. Mobilenets: Efficient convolutional neural networks for mobile vision applications. *arXiv preprint arXiv:1704.04861*.

[Howard et al. 2019] Howard, A.; Sandler, M.; Chu, G.; Chen, L.-C.; Chen, B.; Tan, M.; Wang, W.; Zhu, Y.; Pang, R.; Vasudevan, V.; et al. 2019. Searching for mobilenetv3. *arXiv preprint arXiv:1905.02244*.

[Hu, Shen, and Sun 2018] Hu, J.; Shen, L.; and Sun, G. 2018. Squeeze-and-excitation networks. In *Proceedings of the IEEE Conference on Computer Vision and Pattern Recognition*, 7132–7141.

[Qualcomm 2019] Qualcomm. 2019. Snapdragon neural processing engine sdk. https://developer.qualcomm.com/software/qualcomm-neural-processing-sdk, version: 1.27.1.382.

[Sandler et al. 2018] Sandler, M.; Howard, A.; Zhu, M.; Zhmoginov, A.; and Chen, L.-C. 2018. Mobilenetv2: Inverted residuals and linear bottlenecks. In *Proceedings of the IEEE Conference on Computer Vision and Pattern Recognition*, 4510–4520.

[Srivastava et al. 2014] Srivastava, N.; Hinton, G.; Krizhevsky, A.; Sutskever, I.; and Salakhutdinov, R. 2014. Dropout: A simple way to prevent neural networks from overfitting. *Journal of Machine Learning Research* 15:1929–1958.

[Stamoulis et al. 2019] Stamoulis, D.; Ding, R.; Wang, D.; Lymberopoulos, D.; Priyantha, B.; Liu, J.; and Marculescu, D. 2019. Single-path nas: Designing hardware-efficient convnets in less than 4 hours. *arXiv preprint arXiv:1904.02877*.

[Tan et al. 2019] Tan, M.; Chen, B.; Pang, R.; Vasudevan, V.; and Le, Q. V. 2019. Mnasnet: Platform-aware neural architecture search for mobile. In *Proceedings of the IEEE Conference on Computer Vision and Pattern Recognition*.

[Wu et al. 2019] Wu, B.; Dai, X.; Zhang, P.; Wang, Y.; Sun, F.; Wu, Y.; Tian, Y.; Vajda, P.; Jia, Y.; and Keutzer, K. 2019. Fbnet: Hardware-aware efficient convnet design via differentiableneural architecture search. *The IEEE Conference on Computer Vision and Pattern Recognition (CVPR)*.

[Xiaomi 2018] Xiaomi. 2018. Mobile ai compute engine. https://github.com/XiaoMi/mace, commit hashtag: 03362fa0.

[Yang et al. 2018] Yang, T.-J.; Howard, A.; Chen, B.; Zhang, X.; Go, A.; Sandler, M.; Sze, V.; and Adam, H. 2018. Netadapt: Platform-aware neural network adaptation for mobile applications. In *Proceedings of the European Conference on Computer Vision (ECCV)*, 285–300.

[Zhang et al. 2018] Zhang, X.; Zhou, X.; Lin, M.; and Sun, J. 2018. Shufflenet: An extremely efficient convolutional neural network for mobile devices. In *The IEEE Conference on Computer Vision and Pattern Recognition (CVPR)*.

[Zoph et al. 2018] Zoph, B.; Vasudevan, V.; Shlens, J.; and Le, Q. V. 2018. Learning transferable architectures for scalable image recognition. In *Proceedings of the IEEE Conference on Computer Vision and Pattern Recognition*, 8697–8710.

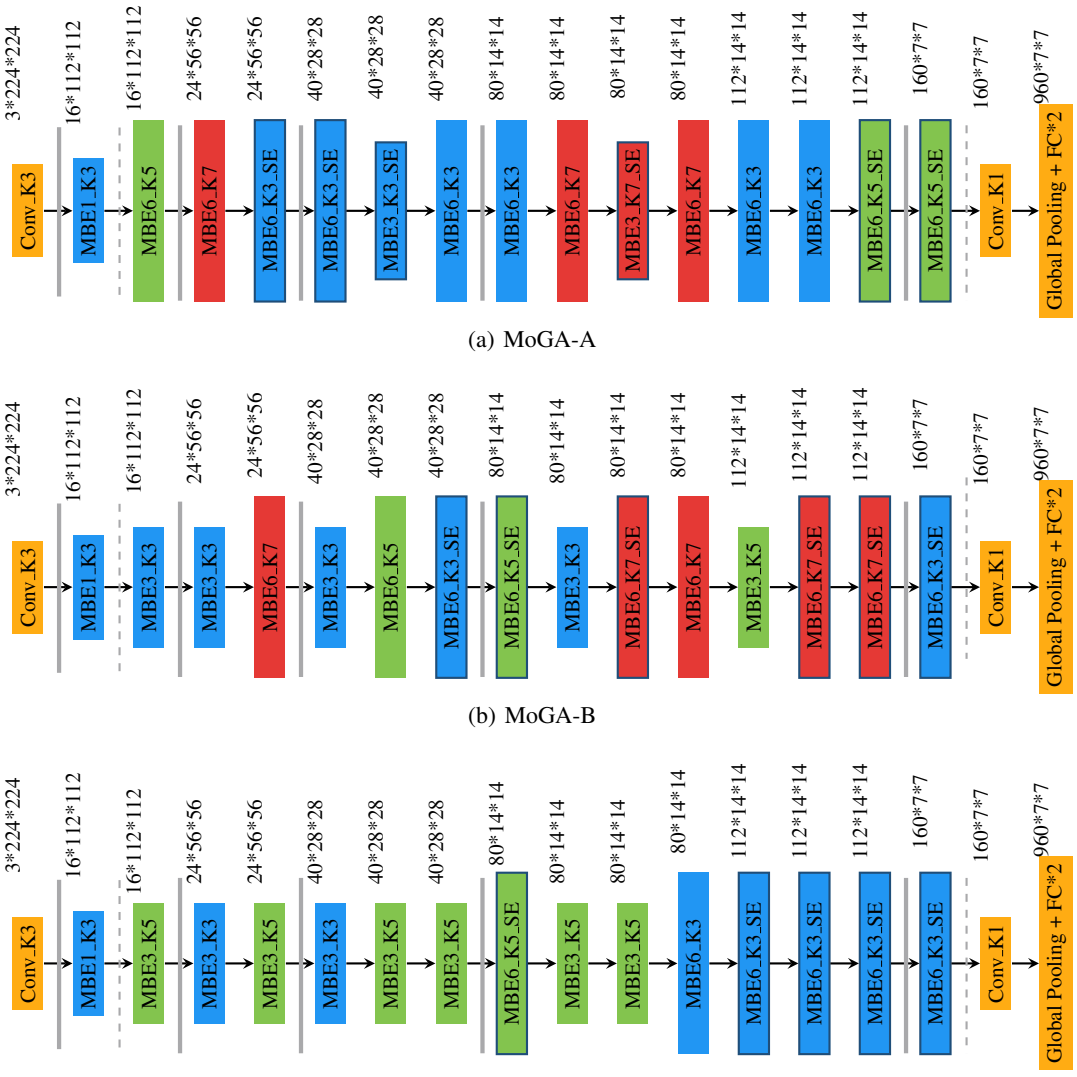

(a) MoGA-A

(b) MoGA-B

(c) MoGA-C

Figure 9: The Architectures of MoGA-A, B, C. Note Ex_Ky_SE means an expansion rate of x for its expansion layer and a kernel size of y for its depthwise convolution layer, SE for squeeze-and-excitation. Grey thick lines refer to downsampling points. Dashed lines separate the stem and end layers from the backbone.